TORSIONAL NATURAL FREQUENCY ANALYSIS OF TORSIONAL VIBRATION DAMPER USING NUMERICAL AND MODAL TEST APPROACHES

Haşmet Çağrı SEZGEN [1], Mustafa TINKIR [2]

[1] KTO Karatay University, Vocational School of Commerce and Industry,
ORCID 0000-0002-6265-4259

[2] Necmettin Erbakan University, Department of Mechanical Engineering,
ORCID 0000-0002-9259-308X

ABSTRACT

This work presents to obtain the torsional natural frequencies and mode shapes of the torsional vibration damper. The torsional vibration damper is mounted on the end of the crankshaft in the opposite direction of the flywheel to dampen the torsional vibrations, especially high-torque diesel engines. The torsional vibration damper used in the study consists of thirteen elements include rubber, silicone and other materials. Therefore, in this study, the Holzer, matrix, finite element methods and modal test are realized to determine the torsional natural frequencies and mode shapes of the proposed torsional vibration damper, then all obtained reaults are compared. The torsional vibration damper, consisting of thirteen elements, is reduced to five masses using the lumped-mass method, and an equivalent lumped mass model is created. This five-mass model is obtained by connecting three masses in series, two masses in series and two masses in series, and three parallel branches. The equations of the motion of the system are achieved using the equivalent model. The obtained equations of motion are used in the determination of torsional natural frequencies using the matrix method. Since the Holzer method is not suitable for the multi-parallel branched lumped-mass model, a modified approach is developed to calculate the system's natural frequencies. For the finite element method, a numerical model of the torsional vibration damper is formed using a one-to-one CAD model. Modal analysis with computer-aided finite element method is carried out with Ansys Workbench software. Finally, the values obtained by performing the modal test are accepted as reference and compared with the values of other numerical methods. Accordingly, the finite element method converged 97%, the matrix method 92% and the Holzer method 90%. Considering the linearization of materials exhibiting nonlinear behavior in the study, the developed modified Holzer method provided a satisfactory convergence.

Keywords: Torsional vibration, Torsional natural frequency, Holzer Method, Modal Analysis, Matrix Method, Finite element Method, Ansys Workbench

1. INTRODUCTION

The aim of this study is to analyze the torsional vibration damper on the cranktrain system operating under dynamic loads. The torsional vibration damper is a part that dampens torsional vibrations and prevents crankshaft fracture and increases fatigue-life. The torsional vibration damper is designed according to the determined vibration characteristics of the cranktrain system. Therefore, the natural frequency and mode shapes of the torsional vibration damper must be determined precisely. Torsional natural frequency values calculated using three different numerical methods and modal tests were compared.

Previous research show that traditional analytical methods, numerical methods, computer aided engineering methods and test methods have been successfully implemented to optimize the torsional vibration damping. For example, a in a study introduced the torsional vibration damper using an innovative method by combining two different parametric optimization methods; energy and modal inertia methods. It has been shown that multi-degree of freedom TVDs provide advantage in parameter optimization, but lose this advantage in low degree of freedom TVDs (Tan et al., 2017). In another related research, presented the torsional vibrations of a crankshaft using two lumped mass mathematical model approaches considering a single mass viscous torsional vibration damper and a double mass rubber TVD. According to the excitation torque map, implications were made about what kind of TVD design should be chosen (Mendes et al., 2008). Torsional vibration dampers can be manufactured from containing rubber-dampers, viscous dampers, or both. Since the mechanical behaviors of rubber and silicone materials do not show a linear elastic, methods specific to the material models should be used in the calculation of stiffness and damping coefficients. The design criteria were determined in order to minimize torsional vibrations of the rubber bearing rotor system driven at different frequencies and, stiffness and damping coefficients were obtained for a realistic lumped mass model (Zhu et al., 2020). When modeling TVD at flexible dynamics methods, the stiffness (k) and damping (c) coefficients of the materials used must be obtained. Viscous and rubber materials, which are elements of TVD, do not exhibit a linear behavior. In a study simplified the geometry using lumped mass model to examine the torsional vibrations of a six-cylinder diesel engine in the crank system and, they obtained critical vibration cycles by Fourier analysis, taking into account firing orders. Generally valid information has been obtained about how much damping effect of TVD in which situations (Mitianiec & Buczek, 2008). Another researcher preferred rubber material as a damping element in TVD models. They compared the torsional vibrations in the crankshaft as 3 models, without TVD, A-type rubber TVD, B-type rubber TVD. Although they did not mention the performance of the B-type rubber damper, they reduced torsional vibrations by approximately 35% (K. Wakabayashi, Y. Honda, T. Kodama, 1995). A rubber material design has been considered to absorb the high amplitudes that occur in the torsional axis during resonance considering the different harmonic orders. According to the results, the torsional vibrations are reduced by approximately 50% with TVD (Ramdasi & Marathe, 2004). In a study, considered the harmonic vibrations, a rubber-type TVD is optimized through AVL software, and the effect of optimization on the stress state caused by torsional vibrations is observed. For comparison, no damper, untuned, tuned unitary and tuned optimum cases are considered and the stress is reduced by approximately 25% (Villalva et al., 2013). In another study mathematically less complex differential equations of the movement of an elastic crankshaft and their solutions with acceptable accuracy according to the actual system have been developed. The instantaneous angular velocity of the free end of the crankshaft consists of solid body motion mode and elastic deformation mode. In general, the crankshaft and other parts of the engine can be modeled as discrete systems. This leads to an infinite number of degrees of freedom and requires the resolution of partial differential equations. Another approach is to separate the continuous system into a series of finitized solid objects that connect with springs and dampers. The partial mass model of the crankshaft and the corresponding motion equations for each mass quite accurately simulate the actual dynamics of the crankshaft (Milašinović et al., 2016).

In this study, they examined the static and dynamic strength of the crankshaft, which is one of the most important components for the effective and precise operation of the internal combustion engine. In this study, a static structural and dynamic analysis has been made on a single cylinder four-stroke diesel engine crankshaft. A suitable model of the crankshaft was created according to the dimensional detail drawings of the existing crankshaft, using advanced computer-aided design software, Pro / Engineer software. Finite element analysis was performed using ANSYS software under static and dynamic conditions to obtain the variation of the stresses of the crankshaft at different critical points. Boundary conditions are applied to the finite element model in accordance with the motor specification scheme and the mounting conditions of the motor. The optimization of the crankshaft has been studied on the existing crankshaft in the area of geometry and shape; However, the optimized crankshaft design, working mainly on geometry and shape optimization, has been replaced by the existing crankshaft without changes in the engine block and cylinder head. The optimized crankshaft helped to improve the performance of the engine and caused a reduction in weight. This optimization study of the crankshaft helped reduce 4.37% of the weight on the original crankshaft (Shahane & Pawar, 2017). In another effort, they performed a breakage, strain and modal analysis of the diesel engine crankshaft. The damaged area was examined by electron microscope and microfractures were detected. The values obtained as a result of the stress tests showed that the material used was within the range defined by the standard. Finite elements method was used to explain the cause of damage to the early fractured crankshaft. When the results of the stress analysis were examined, the maximum stress occurred in a different place from the area where the crack inset occurred. This result showed that there was no static breakage. In the results of modal analysis, it was determined that in the second free vibration mode, the high stress area was located in the crack area. Based on the results of the examinations, it was concluded that the main cause of early fracture was the resonance vibration of the crankshaft (Witek et al., 2017).

2. THE DYNAMIC MODELING OF THE TORIONAL VIBRATION DAMPER

Generally, vibration problems are considered as a single degree of freedom system. But more complex systems can have many degrees of freedom. If the degree of freedom of the system is not more than three, the standard technique used in solving these systems is to obtain equations of motion with Newton's laws of motion. Then the differential equation of motion is solved by assuming a suitable solution. But as the mass number of the system increases, the solution of differential equations becomes almost impossible (Vatandaş, 2017). Considering a system with n degrees of freedom, there are n free vibration equations, which are the 2nd order differential equations, in this system. The frequency equation is obtained as a result of solving these equations and the frequency equation has n roots (Özgür & Pasin, 1996).

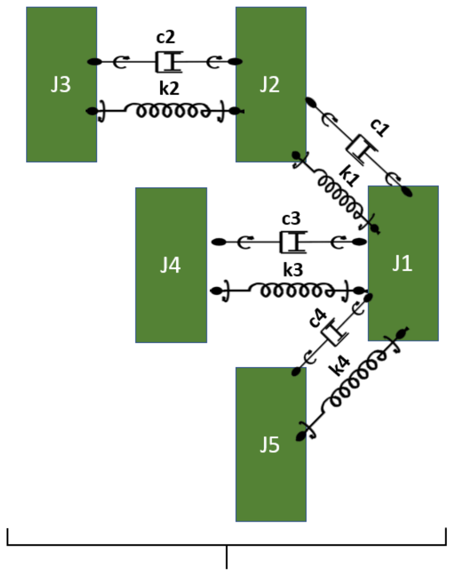

Figure 1 The discrete system model of a double mass rubber and viscous torsional vibration damper

The discrete system model of a double mass rubber and viscous torsional vibration damper (DMRV-TVD) subject to the study is given in Figure 1. DMRV-TVD, which consists of five masses, is obtained by three parallel branches connected in series with each other. Five linear equations belonging to these five masses are obtained. In addition, the parameters of the system, moments of inertia, stiffness coefficients and damping coefficients are also calculated (Sezgen & Tınkır, 2021).

2.1. Holzer, Computer Aided Finite Element, Matrix Method: Undamped Free Vibrations of the Torsional Vibration Damper

For torsional vibration analysis, dunkerley formula, Rayleigh method, Holzer method, Matrix method and Jacobi method were used numerically. As a standard value-value problem, in addition to choleski parsing, many different methods have been used to find a numerical solution to the self-worth problem (Jennings, 1984; Wilkinson, 1965). Bathe and Wilson have compared some of these methods (Bathe & Wilson, 1973). In recent studies, studies have been carried out on methods that can solve complex self-worth problems more simply (Cohen & McCallion, 1967; Fricker, 1983). Studies on obtaining natural frequency values using Sturm arrays (Gupta, 1972). Using topological methods, the discrete system model was presented in an alternative way to solve vibration problems (Chen & Chen, 1969). Computer aided methods and experimental methods are presented in literature research. Double mass rubber and viscous torsional vibration damper, an innovative torsional vibration pulley, have focused on methods that will achieve optimum time, ease of use and accurate result parameters of natural frequency and mode.

1	6.283185	1.34E-02	0.530542	1.00E+00	5.31E-01	5.31E-01	2.53E+04	2.10E-05	12
1	6.283185	7.28E-05	0.002874	0.999979	2.87E-03	5.33E-01			8
1	6.283185	1.07E-02	0.4224191	1.00E+00	4.22E-01	4.22E-01	1.67E+06	2.53E-07	11
1	6.283185	7.28E-05	0.002874	0.9999997	2.87E-03	4.25E-01	1.18E+06		8
1	6.283185	7.28E-03	0.2873856	1.00E+00	2.87E-01	2.87E-01	1.40E+02	2.05E-03	10
1	6.283185	4.96E-04	1.96E-02	0.9979	1.95E-02	3.07E-01	1.03E+06	2.98E-07	9
1	6.283185	7.28E-05	0.002874	0.99795	2.87E-03	3.10E-01			8
1	6.283185	7.28E-03	0.2873856	2.00409	5.76E-01	5.76E-01	1.40E+02	4.11E-03	10
1	6.283185	4.96E-04	1.96E-02	2.0000	3.92E-02	6.15E-01	1.03E+06	5.97E-07	9
1	6.283185	7.28E-05	0.002874	2.0000	5.75E-03	6.21E-01			8
-	-	-	-	-	-	-	-	-	-
-	-	-	-	-	-	-	-	-	-
-	-	-	-	-	-	-	-	-	-
-	-	-	-	-	-	-	-	-	-
-	-	-	-	-	-	-	-	-	-
-	-	-	-	-	-	-	-	-	-
-	-	-	-	-	-	-	-	-	-

Holzer table for first parallel branching

1	6.283185	1.34E-02	0.530542	1.00E+00	5.31E-01	5.31E-01	2.53E+04	2.10E-05	12
1	6.283185	7.28E-05	0.002874	0.999979	2.87E-03	5.33E-01			8
1	6.283185	7.28E-03	0.2873856	1.00E+00	2.87E-01	2.87E-01	1.40E+02	2.05E-03	10
1	6.283185	4.96E-04	1.96E-02	0.9979	1.95E-02	3.07E-01	1.03E+06	2.98E-07	9
1	6.283185	7.28E-05	0.002874	0.99795	2.87E-03	3.10E-01			8
1	6.283185	1.07E-02	0.4224191	1.00E+00	4.22E-01	4.22E-01	1.67E+06	2.53E-07	11
1	6.283185	7.28E-05	0.002874	0.9999997	2.87E-03	4.25E-01	1.18E+06		8
1	6.283185	1.07E-02	0.4224191	1.99793	8.44E-01	8.44E-01	1.67E+06	5.05E-07	11
1	6.283185	7.28E-05	0.002874	1.9979260	5.74E-03	8.50E-01			8
2	12.56637	1.34E-02	2.1221682	1.00E+00	2.12E+00	2.12E+00	2.53E+04	8.39E-05	12

Holzer table for second parallel branching

1	6.283185	7.28E-03	0.2873856	1.00E+00	2.87E-01	2.87E-01	1.40E+02	2.05E-03	10
1	6.283185	4.96E-04	1.96E-02	0.9979	1.95E-02	3.07E-01	1.03E+06	2.98E-07	9
1	6.283185	7.28E-05	0.002874	0.99795	2.87E-03	3.10E-01			8
1	6.283185	1.07E-02	0.4224191	1.00E+00	4.22E-01	4.22E-01	1.67E+06	2.53E-07	11
1	6.283185	7.28E-05	0.002874	0.9999997	2.87E-03	4.25E-01			8
1	6.283185	1.34E-02	0.530542	1.00E+00	5.31E-01	5.31E-01	2.53E+04	2.10E-05	12
1	6.283185	7.28E-05	0.002874	0.999979	2.87E-03	5.33E-01			8
1	6.283185	1.34E-02	0.530542	1.997989	1.06E+00	1.06E+00	2.53E+04	4.19E-05	12
1	6.283185	7.28E-05	0.002874	1.997947	5.74E-03	1.07E+00			8

Holzer table for third parallel branching

Figure 2 Holzer tables for DMRV-TVD

There is no need to derive frequency equations in the Holzer table method (Figure 2). Therefore, it consists of filling in the parameter values in the table for a selected "angular natural frequency" w and observing the final state. When an object vibrates with natural frequency, it can maintain its motion without the need to apply an external torque (M_d) of resonance amplitude. This angular is the main feature that emphasizes the physical meaning of the natural frequency. These amplitudes are arbitrarily shaped according to the size of the first sudden torque pulse we apply in a manner that will drag the torsional system under consideration to free vibration at the natural frequency of that system. For this reason, if the amplitude of one of the masses on the system is assumed to be assigned a certain value as 1, the angular-displacements of the other masses can be easily determined depending on this value. By making use of this property of the amplitudes, it arises that the sum of all internal inertia forces in the system must be zero (Karabay, 2017).

$$\left(-w^2\ nf\cdot\begin{bmatrix} j1 & 0 & 0 & 0 & 0 \\ 0 & j2 & 0 & 0 & 0 \\ 0 & 0 & j3 & 0 & 0 \\ 0 & 0 & 0 & j4 & 0 \\ 0 & 0 & 0 & 0 & j5 \end{bmatrix} + \begin{bmatrix} k1+k3+k4 & -k1 & 0 & -k3 & -k4 \\ -k1 & k1+k2 & -k2 & 0 & 0 \\ 0 & -k2 & k2 & 0 & 0 \\ -k3 & 0 & 0 & k3 & 0 \\ -k4 & 0 & 0 & 0 & k4 \end{bmatrix}\right)\cdot\begin{bmatrix} \theta_1 \\ \theta_2 \\ \theta_3 \\ \theta_4 \\ \theta_5 \end{bmatrix} = \begin{bmatrix} 0 \\ 0 \\ 0 \\ 0 \\ 0 \end{bmatrix}$$

$$w = \begin{bmatrix} 3.116\cdot 10^4 \\ 5.797\cdot 10^3 \\ 321.413 \\ 25.091 \\ 3.723\cdot 10^{-5} \end{bmatrix} \qquad \begin{aligned} j1 &:= 7.28\cdot 10^{-5} \\ j2 &:= 0.000496016 \\ j3 &:= 0.007279563 \\ j4 &:= 0.0107 \\ j5 &:= 0.013438787 \end{aligned} \qquad \begin{aligned} k1 &:= 1.03\cdot 10^6 \\ k2 &:= 140 \\ k3 &:= 1.67\cdot 10^6 \\ k4 &:= 2.53\cdot 10^4 \end{aligned}$$

$$V = \begin{bmatrix} 0.998 & -0.339 & 0.513 & 0.252 & -0.447 \\ -0.057 & -0.94 & 0.514 & 0.252 & -0.447 \\ 2.868\cdot 10^{-8} & 1.362\cdot 10^{-5} & -0.002 & -0.862 & -0.447 \\ -0.004 & 0.045 & 0.527 & 0.252 & -0.447 \\ -4.903\cdot 10^{-5} & 4.823\cdot 10^{-4} & -0.44 & 0.256 & -0.447 \end{bmatrix}$$

Figure 3 Matrix method and parameters of DMRV-TVD

The matrix iteration method assumes that the natural frequencies are distinct and well separated such that $\omega_1 < \omega_2 < \ldots < \omega_n < \omega_n$. The iteration is started by selecting a trial vector $\vec{X}_1$, which is then premultiplied by the dynamical matrix [D]. The resulting column vector is then normalized, usually by making one of its components equal to unity. The normalized column vector is premultiplied by [D] to obtain a third column vector, which is normalized in the same way as before and becomes still another trial column vector. The process is repeated until the successive normalized column vectors converge to a common vector: the fundamental eigenvector. The normalizing factor gives the largest value of $\lambda = 1/\omega^2$ that is, the smallest or the fundamental natural frequency (Mahalingam, 1980). The convergence of the process is explained in Figure 3.

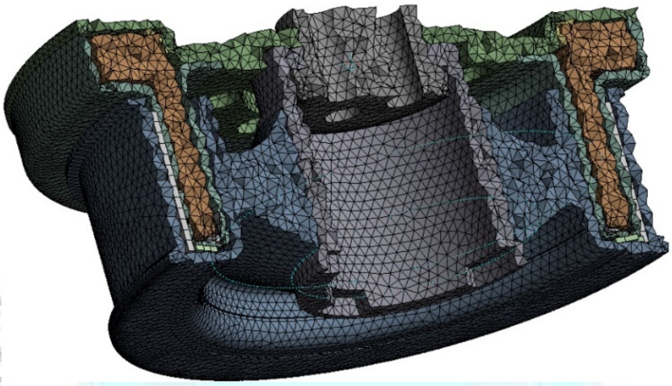

Figure 4 Mesh model of the DMRV-TVD system

Modal analysis, also called frequency analysis, finds natural frequencies and vibration shapes associated with these frequencies. Vibration modes describe a mass that oscillates without damping and forcing forces. While a real-life structure may have an infinite number of degrees of freedom, it still has discrete vibration modes. With its frequency value and associated mode shape, each mode corresponds to the situation where the force due to stiffness is equal to and opposite to the force from inertia (M.Kurowski, 2017).

$$[K].[x] = [F] \quad (1)$$

$$[M]\ddot{x} + [C]\dot{x} + [K]x = [F(t)] \quad (2)$$

where

[M]—mass matrix

[C]—damping matrix

[K]—stiffness matrix

[F]—vector of nodal loads

[x]—vector of nodal displacements

Modal analysis deals with free and undamped vibrations where [F(t)] = 0 (no excitation force) and [C] = 0 (no damping). Therefore, Eq. (2) can be simplified to:

$$[M]\ddot{x} + [K]x = 0 \quad (3)$$

Finding nonzero solutions of Eq. (3) presents an eigenvalue problem; it provides modal frequencies and associated mode shapes of vibration:

$$[K]\{\phi\}_j = \omega_i^2[M]\{\phi\}_j \quad (4)$$

Equation Eq. (4) has n solutions, where ω_i^2 is called the eigenvalue, and the corresponding vector {φ}i is called the eigenvector. The relation between eigenvalue and frequency expressed in Hertz is

$$f_i = \frac{\omega_i}{2\pi} \quad (5)$$

In this study, Ansys software is used to execute the finite element method. Separate material assignment of the parts is made based on a realistic Cad model. Later, connection and boundary conditions are defined to simulate the reality. Another critical issue is determining parametrically a mesh model belonging to the cranktrain system, as shown in Figure 4, to obtain the most accurate result.
In this study, Ansys software is used to execute the finite element method. Separate material assignment of the parts is made based on a realistic Cad model. Later, connection and boundary conditions are defined to simulate the reality. Another critical issue is determining parametrically a mesh model belonging to the cranktrain system, as shown in Figure 4, to obtain the most accurate result.

2.2. Modal Test for Torsional Vibration Damper

Since any dynamic response of a structure can be obtained as a combination of its modes, a knowledge of the mode shapes, modal frequencies, and modal damping ratios constitutes a complete dynamic description of the structure. Experimental modal analysis, also known as modal analysis or modal testing, deals with the determination of natural frequencies, damping ratios, and mode shapes through vibration testing (Brinkman & Macioce, 1985; deSilva & Palusamy, 1984; Dovel, 1989). Two basic ideas are involved:

1. When a structure, machine, or any system is excited, its response exhibits a sharp peak at resonance when the forcing frequency is equal to its natural frequency when damping is not large.
2. The phase of the response changes by 180° as the forcing frequency crosses the natural frequency of the structure or machine, and the phase will be 90° at resonance.

The modal test is used to compare the performance of numerical methods and the results of the modal test were accepted as reference.
The modal test for DMRV-TVD shown in Figure 5 is used to compare the performance of numerical methods, and the results of the modal test have been accepted as reference.

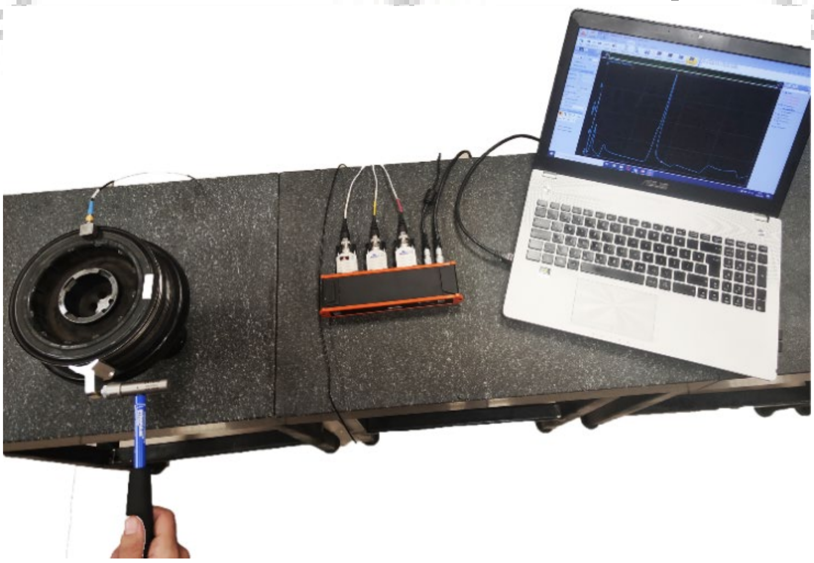

Figure 5 Modal test interface with the DewesoftX software, the accelerometer and modal hammer

While in the actual situation the crankshaft is fixed to the hub, for the DMRV-TVD modal test, a shaft is fixed to the hub. The accelerometer is connected to the pulley part, which is the outer part of the DMRV-TVD. On the same part, a part is attached to the opposite side of the accelerometer to hit it with a modal hammer. The responses of the pulley excited by the modal hammer on the rotary axis are collected from the accelerometer. By connecting the accelerometer and modal hammer to the Dewesoft device, the productive sensitivity values of the accelerometer are entered. After opening the modal test interface with the DewesoftX software, the accelerometer and modal hammer force data are checked. During the test, it is important to operate with a single touch and avoid a double hit from the hammer. After the force from the hammer and the acceleration data from the accelerometer are recorded, the modal frequencies are checked from the FFT Graph.

3. RESULTS AND DISCUSSION

Frequency scanning is performed from one to the end of the working range in the Holzer tables. Values, where total torque is equal to zero, are considered natural frequency. Accordingly, the frequency - total torque graph is drawn, and the natural frequency values are determined. In Figure 6-a and 6-b, the first and second torsional natural frequency values are seen as 23hz. and 307hz. respectively.

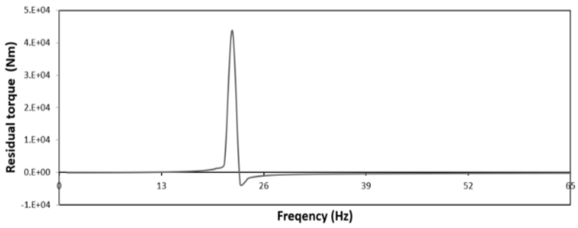

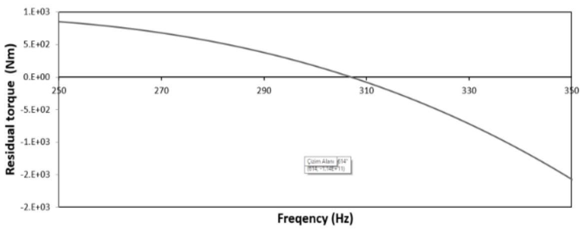

Figure 6 a) First b) Second torsional natural freqency by Holzer method

Finite element modal analysis values expected to be at relative values with the Holzer method. Since the torsional vibration damper has parts that are not visible from the outside, a section has been taken as shown in Figure 7 to understand the mode shapes better. In Figure 7-a, the first torsional natural frequency is found on TVD and about 22,64hz. In Figure 7-b, the second torsional natural frequency value is calculated as 316,28hz.

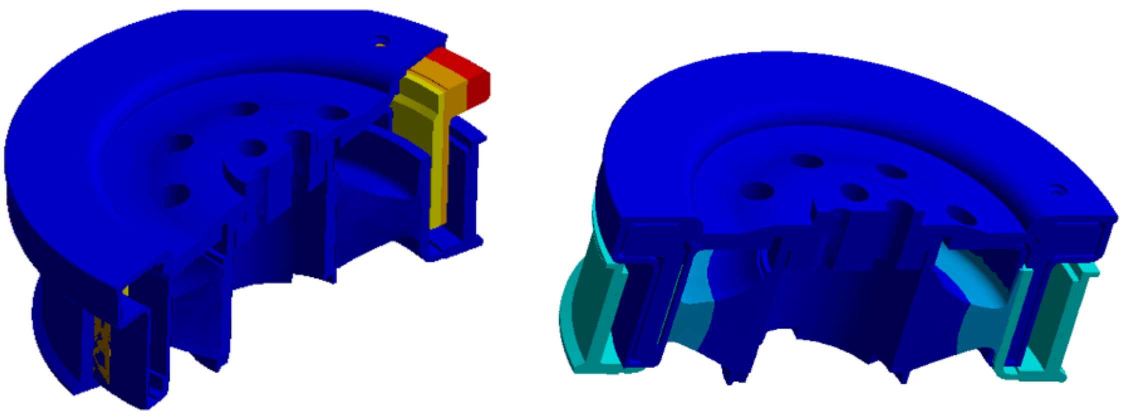

Figure 7 a) First b) Second torsional natural freqency by finite element method

In Figure 8, the first two natural frequency values of 4 different methods are given on the FFT graph. The FFT graph was obtained from the modal test results and transferred to the computer with the DewesoftX software.

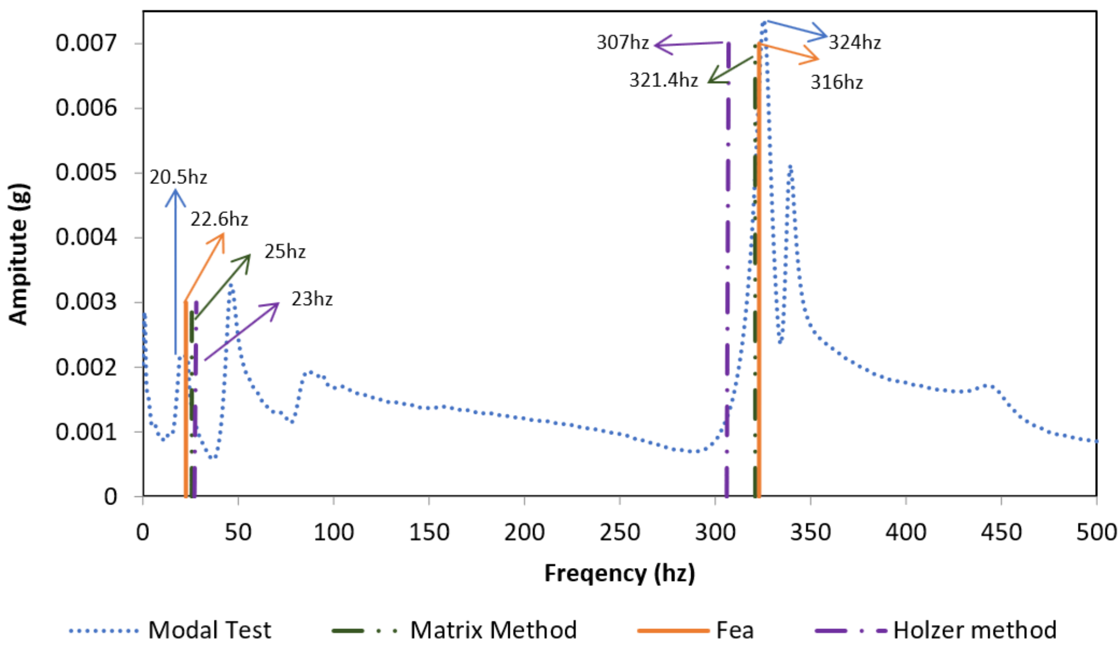

Figure 8 The first two natural frequencies of the 4 methods on the FFT graph

In this table, Holzer, matrix, finite element method and modal test natural frequency results are given comparatively. According to these results, the first natural frequency values calculated by Holzer and matrix methods are relatively far from the reference value. When these methods are considered as simple methods with very few degrees of freedom, they turn out to have very satisfactory results.

Table 1. Method comparison chart

Method	1st torsional natural frequency	Converge	2nd torsional natural frequency	Converge
Holzer Method	23	88%	307	95%
Matrix Method	25,09	78%	321,4	99%
Finite Element Method	22,6	91%	316	97,5%
Modal Test	20,5	referance	324	referance

4. CONCLUSIONS

According to these results, the first natural frequency values calculated by Holzer and matrix methods are relatively far from the reference value. When these methods are considered as simple methods with very few degrees of freedom, they turn out to have very satisfactory results.

5. REFERENCES

Bathe, K. -J, & Wilson, E. L. (1973). Solution methods for eigenvalue problems in structural mechanics. *International Journal for Numerical Methods in Engineering*.

Brinkman, B. A., & Macioce, D. J. (1985). UNDERSTANDING MODAL PARAMETERS AND MODE SHAPE SCALING. *S V Sound and Vibration*.

Chen, W. K., & Chen, F. Y. (1969). Topological analysis of a class of lumped vibrational systems. *Journal of Sound and Vibration*.

Cohen, E., & McCallion, H. (1967). Economical methods for finding eigenualues and eigenvectors. *Journal of Sound and Vibration*.

deSilva, C. W., & Palusamy, S. S. (1984). EXPERIMENTAL MODAL ANALYSIS - A MODELING AND DESIGN TOOL. *Mechanical Engineering*.

Dovel, G. (1989). Modal analysis: A dynamic tool for design and troubleshooting. *Mechanical Engineering*.

Fricker, A. J. (1983). A method for solving high-order real symmetric eigenvalue problems. *International Journal for Numerical Methods in Engineering*.

Gupta, K. K. (1972). Solution of eigenvalue problems by sturm sequence method. *International Journal for Numerical Methods in Engineering*.

Jennings, A. (1984). Eıgenvalue Methods For Vıbratıon Analysıs. Iı. *Shock And Vibration Digest*.

K. Wakabayashi, Y. Honda, T. Kodama, K. S. (1995). Torsional vibration damping of diesel engine with rubber damper pulley. *JSME Int. J. Series C*, *38*(4), 670–678.

Karabay, S. (2017). *Mekanik Titreşimler*. Birsen Yayınevi.

M.Kurowski, P. (2017). Finite Element Analysis for Design. In *Journal of Physics A: Mathematical and Theoretical* (Vol. 44, Issue 8).

Mahalingam, S. (1980). Iterative procedures for torsional vibration analysis and their relationships. In *Journal of Sound and Vibration*.

Mendes, A. S., Meirelles, P. S., & Zampieri, D. E. (2008). Analysis of torsional vibration in internal combustion engines: Modelling and experimental validation. *Proceedings of the Institution of Mechanical Engineers, Part K: Journal of Multi-Body Dynamics*, *222*(2), 155–178.

Milašinović, A., Milovanović, Z., Knežević, D., & Mujanić, I. (2016). Determination of differential equations of motion and parameters of an elastic internal combustion engine crankshaft. *Transactions of Famena*, *40*(2), 83–95.

Mitianiec, W., & Buczek, K. (2008). Torsional Vibration Analysis of Crankshaft in Heavy Duty Six Cylinder Inline Engine. *Czasopismo Techniczne. Mechanika*, *R. 105*, z. *8–M*, 193–207.

Özgür, K., & Pasin, F. (1996). Separation phenomena in force closed cam mechanisms. *Mechanism and Machine Theory*.

Ramdasi, S. S., & Marathe, N. V. (2004). Predictive-Cum-Experimental Analysis of Torsional / Bending and Crankcase Vibrations and Design of Optimum Tuned Damper. *SAE Technical Papers*, *2004-Janua*(January).

Sezgen, H. Ç., & Tınkır, M. (2021). Optimization of torsional vibration damper of cranktrain system using a hybrid damping approach. *Engineering Science and Technology, an International Journal*.

Shahane, V. C., & Pawar, R. S. (2017). Optimization of the crankshaft using finite element analysis approach. *Automotive and Engine Technology*, *2*(1–4), 1–23.

Tan, X., Hua, L., Lu, C., Yang, C., Wang, Y., & Wang, S. (2017). A new method for optimizing the parameters of torsional vibration dampers. *Journal of Vibroengineering*, *19*(6), 4155–4171.

Vatandaş, S. (2017). Gemi Şaft Sistemi Burulma Doğal Frekanslarının Holzer Metodu Algoritması İle Tespit Edilmesi. In *Fen Bilimleri Enstitüsü*. İstanbul Teknik Üniversitesi.

Villalva, S. G., Bittencourt, M. L., & Zampieri, P. R. (2013). Methodology for automotive crankshaft design using analytical and flexible models. *SAE Technical Papers*, *13*.

Wilkinson, J. H. (1965). The Algebraic Eigenvalue Problem Oxford University Press. *New York*.

Witek, L., Stachowicz, F., & Załęski, A. (2017). Failure investigation of the crankshaft of diesel engine. *Procedia Structural Integrity*, *5*, 369–376.

Zhu, H., Chen, W., Zhu, R., Gao, J., & Liao, M. (2020). Study on the Dynamic Characteristics of a Rotor Bearing System with Damping Rings Subjected to Base Vibration. *Journal of Vibrational Engineering and Technologies*, *8*(1), 121–132.